Influence of Molecular Dipole Orientations on Long-Range Exponential Interaction Forces at Hydrophobic Contacts in Aqueous Solutions

Kai Kristiansen,[†] Philipp Stock,[‡] Theodoros Baimpos,[‡] Sangeetha Raman,[‡] Jaye K. Harada,[§] Jacob N. Israelachvili,*[,†,∥] and Markus Valtiner[‡]

[†]Department of Chemical Engineering, [§]Materials Research Laboratory, and [∥]Materials Department, University of California, Santa Barbara, California 93106, United States and [‡]Department of Interface Chemistry and Surface Engineering, Max-Planck-Institut für Eisenforschung GmbH, D-40237 Düsseldorf, Germany

ABSTRACT Strong and particularly long ranged (>100 nm) interaction forces between apposing hydrophobic lipid monolayers are now well understood in terms of a partial turnover of mobile lipid patches, giving rise to a correlated long-range electrostatic attraction. Here we describe similarly strong long-ranged attractive forces between self-assembled monolayers of carboranethiols, with dipole moments aligned either parallel or perpendicular to the surface, and hydrophobic lipid monolayers deposited on mica. We compare the interaction forces measured at very different length scales using atomic force microscope and surface forces apparatus measurements. Both systems gave a long-ranged exponential attraction with a decay length of 2.0 ± 0.2 nm for dipole alignments perpendicular to the surface. The effect of dipole alignment parallel to the surface is larger than for perpendicular dipoles, likely due to greater lateral correlation of in-plane surface dipoles. The magnitudes and range of the measured interaction forces also depend on the surface area of the probe used: At extended surfaces, dipole alignment parallel to the surface leads to a stronger attraction due to electrostatic correlations of freely rotating surface dipoles and charge patches on the apposing surfaces. In contrast, perpendicular dipoles at extended surfaces, where molecular rotation cannot lead to large dipole correlations, do not depend on the scale of the probe used. Our results may be important to a range of scale-dependent interaction phenomena related to solvent/water structuring on dipolar and hydrophobic surfaces at interfaces.

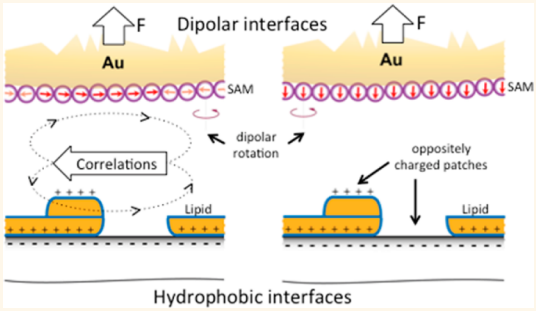

KEYWORDS: molecular dipole · hydrophobic · self-assembled monolayer · surface forces apparatus

Variation of surface chemistry provides a powerful lever for tailoring interactions between apposing surfaces in the wide range of living and engineering systems. In biological and biomedical systems for instance, specific chemical interactions (*e.g.*, ligand−receptor interactions) and nonspecific interactions (*e.g.*, H-bonding and hydrophobic interactions) control functionality and stability of cell|surface,[1] protein|surface,[2] and serum|biomaterial interactions, among many others. A large range of available surface chemistries can be used for tailoring drug-carrier interactions with cell membranes.[3] Also, adhesives used for tissue gluing[4] or adhesion promotors used in organic coatings for metal surfaces utilize chemical functionalities of catechols[5] or phosphonates[6] in order to increase bonding stability of an adhesive joint. In addition, not only increased but also lowered interactions can be tailored directly by adjusting interfacial chemistries and steric interactions between interacting surfaces. In most technological tailoring solutions, chemical interactions and steric repulsion are utilized and a direct tailoring of surface chemistry and interfacial interaction forces is straightforward.[7]

Self-assembled monolayers of *n*-alkanethiols,[8] *n*-alkanesilanes,[9] and organo-phosphonates[10] are among the most widely studied systems to directly vary chemical properties of metal and oxide surfaces. Yet, chemical variation in many cases also

* Address correspondence to jacob@engineering.ucsb.edu.

Received for review August 20, 2014 and accepted October 7, 2014.

Published online October 07, 2014
10.1021/nn504687b

results in a variation of the interfacial dipole moment. Decoupling of chemical effects and effects due to interfacial dipoles is not straightforward, mainly because of the inability to vary the dipole moment independent of the applied chemical variations. Yet, surface dipoles and alignment of solution side dipoles are fundamental to a range of interaction forces. In particular, interaction forces across water between two hydrophobic surfaces may be related to an alignment of water dipoles at hydrophobic interfaces, which has been controversially discussed in the past.[11−15]

Recently, Hohman *et al.*[16,17] produced chemically identical and quite hydrophobic surfaces with strongly varying dipole moments using carborane-based self-assembled monolayer chemistry. Here, we quantify the effect of the variation of surface dipole moments on range and magnitude of interaction forces between these carborane-based self-assembled monolayers and apposing hydrophobic lipid monolayer surfaces.

Figure 1 shows a schematic of the used setup and chemical surface modification. We use the surface forces apparatus (SFA) and atomic force microscopy (AFM) together to study the scaling of the involved interaction forces with varying contact radii ranging from a few nanometers to centimeters. We utilize self-assembled monolayers (SAM) of the two carborane isomers 1-mercapto-1,7-dicarba-closo-dodecaborane (m-1-carboranethiol, henceforth **M1**) and 9-mercapto-1,7-dicarba-closo-dodecaborane (m-9-carboranethiol, henceforth **M9**). The dipole moments of the precursor molecules **M1** and **M9** are aligned perpendicular or parallel to the surface after formation of the SAM (see inset in Figure 1). Using this setup, the influence of the interfacial dipole moment on range and magnitude of interaction forces can be studied in detail. Here we focus on the interaction with extended apposing hydrophobic surfaces across water. However, the setup shown in Figure 1 may be extended for studying the influence of surface dipoles on a wide range of systems including adsorption of polymers at interfaces or interfacial ion-layering in (non)aqueous solutions and ionic liquids.

RESULTS AND DISCUSSION

Direct quantification of the interaction forces between self-assembled monolayers of **M1** (or **M9**) carboranethiols and hydrophobic DODA lipid monolayers shows strong influence of the dipole moment alignments parallel (or perpendicular) to the surface. It is interesting to note that molecular rotation of the carboranethiol molecules perpendicular to the surface (along the sulfur gold bond axis) changes the direction of the dipole moments for the **M1** molecules only, while the rotation of **M9** molecules does not vary the dipole moment direction (see again Figure 1, inset). The **M1** SAM may therefore display correlation effects, such as dynamic alignment of surface dipoles in registry and in feedback with an approaching surface that will alter the interaction forces. Chemically the two SAMs are very similar, and for both SAMs boron atoms are facing the solution (opposite side of the sulfur−gold bond). The advancing and receding water contact angles of **M1** and **M9** monolayers are reported to be 82° ± 2° and 71° ± 1°, and 72° ± 4° and 52° ± 1°, respectively,[16] and as such both SAMs have a considerable hydrophobic character.[16] We measure the advancing and receding contact angles of 86° and 70°, and 81° and 53° for **M1** and **M9**, respectively. Water contact angle hysteresis often stems from hydration of the SAM layer, which usually lowers the solid−liquid interfacial tension and therefore reduces the receding contact angle compared to the advancing.[18] The different acidity of the upward oriented hydrogen atoms of **M1** and **M9** molecules may cause different surface charging and hydration, and hence the observed difference in the behavior of the receding contact angles.[16]

X-ray photoelectron spectroscopy (XPS) measurements of **M1** and **M9** surfaces, Figure 2 and Supporting

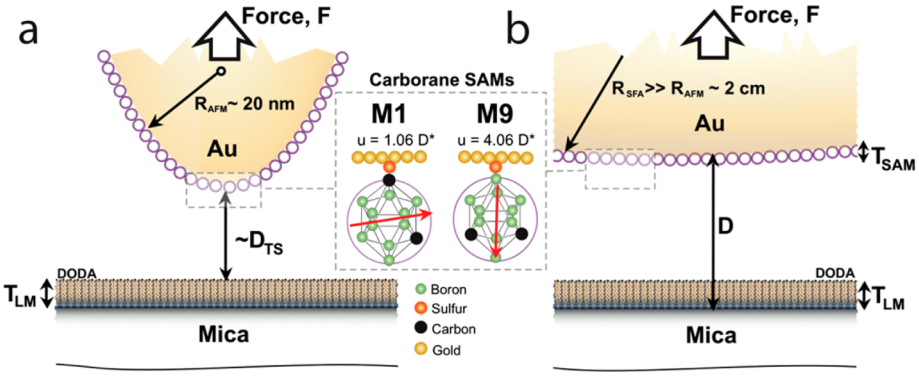

Figure 1. Schematic of the experimental system. Ensuing force *versus* distance characteristics using (a) AFM and (b) SFA experiments with gold probes modified with carborane self-assembled monolayers were measured against hydrophobic DODA lipid monolayers grafted on mica in different salt concentrations at pH 5.5. The thickness of the DODA monolayer T_{LM} and the carborane SAM T_{SAM} are indicated.

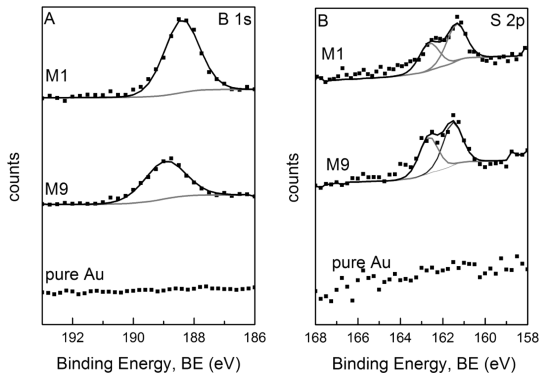

Figure 2. (A) B 1s and (B) S 2p XPS fine spectra of M1, M9, and pure gold samples as indicated.

Information Table S1, show that they are chemically identical. Moreover, the XPS measurements indicate good surface quality of both carborane SAMs on gold. The B 1s signal indicates a shift to higher binding energies for the **M9** compared to the **M1** SAM, which is consistent with a higher work function due to the perpendicular dipole moment at the surface. Both **M1** and **M9** indicate a complete and stable SAM formation with S 2p binding energies at 162.6 eV, as well as the expected $P_{1/2}$ and $P_{3/2}$ ratio of 2:1 indicating that sulfur is covalently bound to gold and no unbound molecules are present. Also, the XPS results are in good agreement with previously published data of a closely related carborane system.[19] On the basis of the XPS data, the two SAM surfaces are chemically identical, while physically they are different by the orientation of the dipole moment only.

Figure 3 shows force distance characteristics measured between carboranethiol-modified gold surfaces facing either a hydrophobic dimethyldioctadecylammonium (DODA) lipid monolayers on mica or bare mica (as indicated). All measurements were done in KCl solutions at pH 5.5. These force−distance profiles indicate several significant differences in the long-range forces of the two SAM surfaces.

The force distance characteristics of approaching surfaces for **M1** SAMs show strong attractive forces with a very abrupt jump-in; that is, the attractive surface forces overpower the restoring cantilever spring forces and rapidly (less than 0.5 s) impel the surfaces together into a direct flat contact. It is interesting to note that the jump-ins are sometimes instantaneously fast and capable of trapping water between the contacting surfaces (indicated in Figure 3). After a sudden instability jump-in, successive layers of water molecules are forced to flow out from between the two surfaces within a few seconds, which can be directly observed from the fringes of equal chromatic order (FECO) in the SFA.[20,21] Most of the trapped ions will flow out together with the water, as the ionic diffusivity between two surfaces separated by a few water molecule layers are similar to the ionic diffusivity in

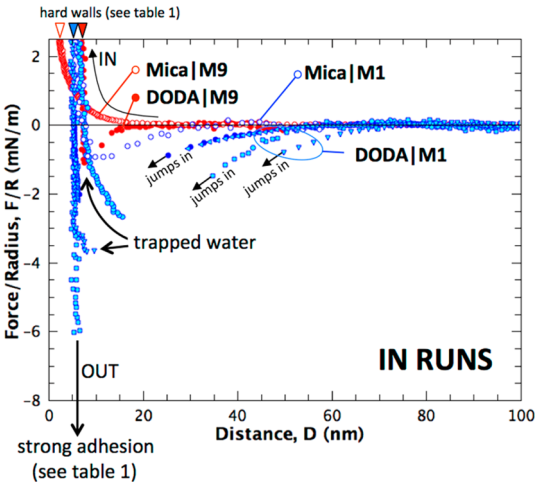

Figure 3. Ensuing force-distance characteristics between M1 or M9-modified gold surfaces facing hydrophobic supported DODA lipid monolayers on mica or bare mica (as indicated) measured in SFA in KCl solutions at pH 5.5 (cf., text for details). All in-run profiles for the M9 SAM do not depend on the solution concentration, while force profiles of the M1 SAM facing DODA display a dependence on the solution concentration. In particular, at higher concentrations the jump-in distance is further in, while the decay length is around 2 nm for all cases. The adhesion varies strongly with the salt concentration and is tabulated in Table 1.

bulk water.[22] Surprisingly, the jump-ins occur at distances much greater than expected from conventional theories of interfacial forces, such as the well-known theory of Derjaguin, Landau, Verwey, and Overbeek (DLVO).[23] Hence, we do not attempt to fit DLVO to these force profiles.

The jump-in distance of the **M1** SAM depends on the screening length of the used electrolyte. In particular, in 1 mM solution concentrations the jump-in occurs at $D \approx 40-50$ nm, in 10 mM solution at $D \approx 30$ nm, and in 100 mM solutions at $D \approx 20$ nm. The observed screening of the jump-in distance of **M1** surfaces may be explained as screening of dipole interactions similar to the van der Waals interaction. The electrostatic screening of the long-ranged dipolar electrostatic interaction is then similar in nature to the screening of the nonretarded Hamaker constant $A_{\nu=0}$ of the van der Waals forces: $A \approx A_{\nu=0}\ e^{-\kappa D} + A_{\nu>\nu 1}$, where A is the total Hamaker constant, $A_{\nu>\nu 1}$ is the retarded Hamaker constant, and κ is the Debye length.[23] Before surfaces jump into direct contact, the force profile is exponentially attractive, with a typical exponential decay length of 9.5 ± 0.5 nm in 1 mM KCl. This indicates that an electrostatic interaction that is extremely strong yet screened with the Debye length may be the physical origin of this surprisingly long-ranged attraction. Again, electrostatic interactions due to overlapping electric double layers formed on charged surfaces cannot explain or fit the observed long-range forces in these systems.[23]

A similar electrolyte-dependent effect of the jump-in distance has been observed between two interacting

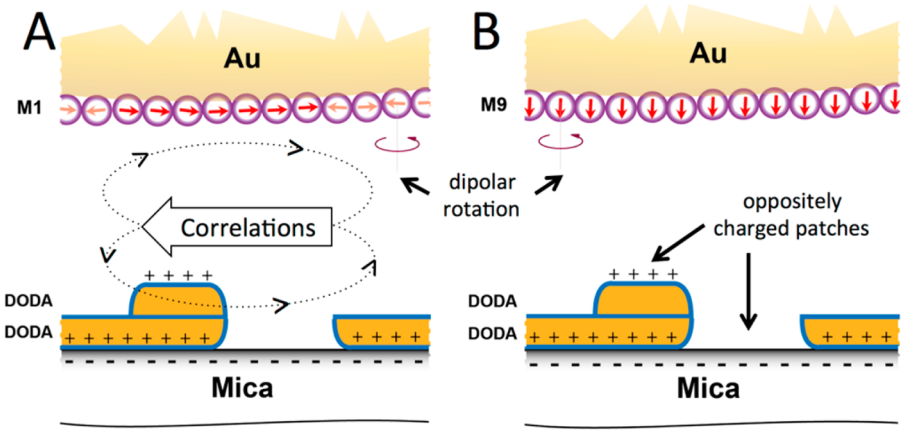

Figure 4. Schematic of possible scenarios during the interaction of carboranethiol SAMs and DODA monolayers. (A) Molecular rotation of the M1 dipole around the Au−S bond may lead to lateral correlation of M1 dipoles within the surface plane. Correlation between such generated giant dipoles and charge patch defects (lipid turnover) on the DODA monolayer may lead to long-range attraction. (B) M9 SAMs cannot exhibit lateral correlation of dipoles within the film. Rotation of M9 around the Au−S bond does not change the direction of the dipole. The rotation axis is indicated (cf., text for details).

lipid monolayers in aqueous media.[14,15] However, it was found that the lipid monolayers undergo overturning[24] that create patches of a positively charged bilayer, leaving behind a negatively charged free substrate (*i.e.*, mica is negatively charged at pH 5.5). As a consequence the lipid patches rearrange into a correlated state of charged domains of positive and negative character that leads to an unexpectedly long-range electrostatic interaction ranging over 50−100 nm.

The monolayer of DODA of the present experiments may similarly create bilayer patch defects and hence a mosaic of positively and negatively charged areas at the interface (see Figure 4A). These patches can then form large electric dipoles parallel to the surface that may interact strongly with the apposing **M1** surface. In addition, the molecular rotations of **M1** molecules around the sulfur−gold bond can correlate with the apposing dipoles of the DODA surface and form similarly large (giant) dipoles of **M1** molecules parallel to the surface. During approach of **M1** and DODA surfaces, the simultaneous correlation of dipoles of the apposing surfaces can lead to a long-range electrostatic correlation and enhance the attraction (see again Figure 4A). As such, the mechanism for the long-range force observed in our experiments is very similar to two lipid monolayers interacting,[14,15] and is apparently based on a large-scale (lateral) electric dipole correlation across the interacting apposing surfaces.

In contrast to the behavior of the **M1** SAM, force distance profiles recorded for the **M9** SAM show no unexpected jump-in at large separation distances. Rotations of **M9** molecules around the Au−S bond do not change the dipole direction (see Figure 4B), and hence no giant dipole similar to the **M1** SAM can be formed that can interact with a possible dipole at the DODA surface. Here, jump-in occurs at distances of about $D \approx 8-10$ nm with respect to the plane of origin, and force-distance profiles indicate an exponential attraction with a typical decay length of 1.9 ± 0.2 nm, which is independent of the solution concentration. This interesting behavior indicates that there is no long-ranged electrostatic correlation between the **M9** SAM and the DODA lipid monolayer (*i.e.*, long-ranged electrostatic attraction would scale with the Debye length and hence concentration of the solution).

Yet, the jump-in distance is longer than that expected from pure van der Waals (VDW) forces. Compared to the typically observed instabilities at $D \approx 15-18$ nm found for two apposing hydrophobic surfaces using SFA,[12,25−28] the jump-in occurs at slightly longer distance. Taking into account the weak hydrophobic character of the **M9** SAM, with a contact angle of 72° ± 4°, this indicates that an additional exponential attraction similar to a hydrophobic attraction is present, and might be due to water structuring at the interface.

Interestingly, the decay length of this additional exponential attraction force is 1.9 ± 0.2 nm for the **M9** SAM, and hence a much longer range compared to that of interactions of pure hydrophobic surfaces, which have a decay length of 1.0 ± 0.1 nm.[25,27] This increased decay length may indicate that the interfacial dipole alignment (*i.e.*, the alignment of water molecules with the surface dipole of the **M9** SAM surface) may lead to an entropically unfavorable longer ranged ordering of water. Hence a dipole-induced solvent layering at the interface may mediate the longer ranged force—a striking conceptual similarity to purely hydrophobic forces. However, this solvent mediated attractive force may be amplified (also act over longer distance range) due to an additional bias from the molecular dipole moments of the carborane SAM.

For both cases, **M1** or **M9** SAMs facing DODA lipid monolayers, the adhesion varies strongly with the salt concentration as tabulated in Table 1. The adhesion

TABLE 1. Work of Adhesion W_{ADH} (mJ/m^2) and Hardwall Distances D_{HW} (nm) of SFA Data Shown in Figure 3

systems	concentration (mM) pH 5.5	work of adhesion W_{ADH} (mJ/m^2)	hardwall distance D_{HW} (nm)
DODA|M1	1 mM	49 ± 7	5.2 ± 0.5
DODA|M1	10 mM	24 ± 3	5.2 ± 0.5
DODA|M1	100 mM	12.8 ± 2.7	5.2 ± 0.5
Mica|M1	1 mM	9.6 ± 0.6	1.8 ± 0.3
Mica|M1	10 mM	12.9 ± 2.1	1.9 ± 0.3
Mica|M9	1 mM	no adhesion	1.5 ± 0.3
Mica|M9	10 mM	no adhesion	1.7 ± 0.3
DODA|M9	1 mM	44 ± 3	6.2 ± 0.5
DODA|M9	100 mM	15.5 ± 1.4	7.2 ± 0.5

energy between two hydrophobic surfaces is generally only weakly dependent on electrolyte concentration; however, the morphology of the patches of the lipid mono- and bilayer will change with the concentration (and ionic type). Any change in the lipid mono- and bilayer morphology has impact on the adhesion energy.

Figure 3 also shows that measurements of **M1** and **M9** SAMs facing a hydrophilic mica surface gives completely different force−distance profiles compared to when the carborane surfaces faces the hydrophobic DODA surface. The **M1** SAM shows a shallow attractive force with a mica surface and only a weak adhesion, while the **M9** SAM shows a purely repulsive interaction, and no adhesive minimum (see Table 1).

As discussed above, in-plane rotational alignment and correlation of electric dipoles across an extended interface lead to an unexpected long-range attraction for the **M1** SAM. To study the influence of contact area on the long-range behavior, we repeated the study using gold-coated AFM tips coated with carboranethiol (see again Figure 1A). The AFM tips used here typically were round-shaped gold grain tips with radii ranging from 8 to 40 nm[29] (for SEM pictures see, *e.g.*, ref 1).

Figure 5 shows typical ensuing force *versus* distance profiles recorded for either an **M1** or **M9** SAM facing a DODA monolayer in 1 mM NaCl. The small inset shows a histogram of the measured adhesion.

The force−distance curves shown in Figure 5 indicate no long-range electrostatic repulsive force with an expected Debye length of λ_D = 9.6 nm for both **M1** and **M9** coated tips. However, both **M1** and **M9** show a long-ranged exponential attraction with a decay length of λ_{Hy} = 2 nm, which interacts as a superposition to the ever-present van der Waals forces. The measured data are fitted to eq 1 (see details in the Materials and Methods section), and the parameters for each fit are given in the caption of Figure 5. The AFM results of the **M9** functionalized tips agree very well with the SFA data. In contrast, the AFM experiments with **M1** coated tips indicate weaker attraction with the DODA monolayer compared to the SFA measurements, but they still

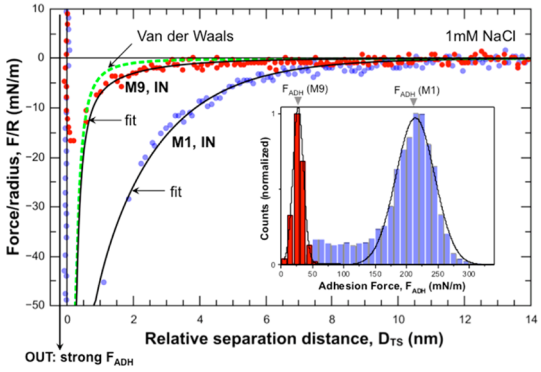

Figure 5. AFM approach curves and data fit showing VDW in comparison to fitting eq 1 using a linear superposition of VDW forces and a generalized hydration in terms of the Hydra parameter.[25,28] For consistency, Hydra was set to Hy = 1 for both SAMs, leading to $\gamma_i \approx$ 100 mJ/m^2 and $\gamma_i \approx$ 10 mJ/m^2 for M1 and M9, respectively. These numbers have to be taken with a grain of salt, as the AFM probe radius is not known with good accuracy in this case. For both M1 and M9 the decay length fits well with about λ_{Hy} = 2 nm, which is independent of the tip radii. The small inlet shows the histogram plots of the measured adhesion forces.

show the expected long-range attractions. The contact area with AFM tips ($R \approx$ 20 nm) are 3 orders of magnitude lower than the contact area with an SFA. In addition, the nanoscopic radius of AFM tips prevents any long-range lateral correlations with the hydrophobic DODA monolayer. Comparing the SFA and AFM data of the **M1** SAM facing the DODA monolayer supports the hypothesis that laterally large-scale electrostatic correlations mediate the long-range attraction at extended contact areas (as used in SFA), while such long-range correlations are not possible in the AFM experiment.

In addition, the adhesion measured with the AFM for the two carboranethiol SAMs is considerably different (see Figure 5). First, the adhesion force histogram of the **M9** SAM shows a Gaussian shape, while the adhesion of the **M1** SAM shows a Gaussian shape together with a weak but pronounced second Gaussian at much lower adhesion forces. The AFM adhesion forces were measured in a grid with step sizes of 100 nm over an area of 1 × 1 μm^2. Hence also local variations of the surface chemistry are reflected in the AFM measurement. A large fraction of the surface is hydrophobic, while about 10−15% of the surface area shows an extra attractive force, which is likely due to charge patches of overturned lipid molecules (see Figure 4). Second, in both experimental methods the adhesion of the **M9** SAM is slightly weaker than that of the **M1** SAM, (though the difference is less pronounced in the SFA measurements). We attribute this to the different radii used in the AFM experiments. The radius of the probes used can vary from 8 to 40 nm, and as such larger relative errors are expected for adhesion measurements using AFM.

In general, for both **M1** and **M9** SAMs AFM force distance profiles reveal an additional exponential force

that can be well fitted using the Hydra model[12,25,28] (see the methods section) with a decay length of λ_{Hy} = 2 nm. As discussed above, this may be due to the preferential orientation of water dipoles in line with the surface dipoles of the SAM molecules. A back of an envelope calculation (see Supporting Information) indicates that carborane-dipole/water-dipole interactions are on the order of 1 kT, which is comparable to the energy that gives rise to the Brownian motion. Hence a time-averaged and biased dipole orienting of water dipoles in line with the carborane dipoles may be expected.

While we consistently find that the **M1** SAM shows a stronger attraction compared to the **M9** SAM, the differences in magnitude (the fitted Hy parameter of eq 1) for both SAMs may be to a large extent a radius normalization problem typical to AFM. Regardless of the absolute numbers, these data indicate that alignment of interface dipoles (*i.e.*, water) by surface dipoles can lead to a long-range exponential attraction. This is conceptually very similar to hydrophobic interactions. However, at purely hydrophobic interfaces dipole alignment is entirely controlled by the thermodynamics of the solution-side hydrogen bond-bridging network and the weak and nondirectional binding of water to hydrophobic interfaces that lead to a water or hydrogen bonding network depletion zone.[30] In the present case, surface dipoles present an additional bias and alignment restriction, and may hence directly lead to an enhanced layering of water and hence longer decay length compared to hydrophobic attractions, which have a decay length of about 1 nm.[11,25−28,31] As such these results may contribute further to the understanding of the interplay between surface chemistry, surface dipole moments, and the observed hydrophobic/hydrophilic interactions between apposing surfaces.

CONCLUSIONS

In summary, we showed that interfacial dipoles together with scaling have a profound effect on interaction forces across aqueous media. First, alignment of dipoles perpendicular or parallel to the surface leads to a long-ranged exponential attraction with a decay length of 2 nm between interacting hydrophobic surfaces, potentially due to biased entropically unfavorable solvent alignment at the interface. The effect of parallel alignment is generally larger, potentially due to lateral alignment of surface dipoles into effectively much larger giant dipoles. Similarly, with extended surfaces, the dipole alignment parallel to the surface leads to an unexpected long-range attractive force due to electrostatic correlations of freely rotating surface dipoles and charge-mosaic defects (partial lipid turnover) on the apposing lipid monolayer surfaces. In contrast, perpendicular dipole alignments, where molecular rotation cannot lead to lateral long ranged dipole correlations, is independent of the scale of the probe used.

As such, alignment of interfacial dipoles may provide a strategy to achieve strong and long ranged attractive forces and adhesion in aqueous systems—an effect that has not been considered in detail so far. Our results also suggest that switching dipole orientations *in situ* may be a valuable tool for responsive materials.

MATERIALS AND METHODS

Chemicals and Materials. **M1** and **M9** carboranethiols and all solvents were purchased from Sigma-Aldrich at the highest available purity and were used as received. Lipids were purchased from AvantiLipids. Milli-Q (Millipore) water with a resistivity of ≤18 $\mu\Omega$-cm and a TOC below 2 ppb was used for the preparation of the NaCl-solutions. The pH value was between 5.5 and 5.7 for all solutions.

Atomic Force Microscopy (AFM). All AFM measurements were performed with a JPK NanoWizard using gold-coated silicon tips (CONTGB-G, BudgetSensors). The sensitivity of the piezo of the AFM (Nanowizard, JPK Instruments, Germany) was measured through several force plots on the SAM−surface. The cantilever with self-assembled monolayer was calibrated to estimate its spring constant using a thermal noise method. Typically the spring constants of different cantilevers varied from 250 to 500 pN/nm. The tip sample distance D_{TS} in AFM is relative, and the apparent hardwall at the maximum compression is calibrated as D = 0. Additionally we want to note that the radius normalization was done using the average tip radius of R = 20 nm given by the supplier.

AFM Tip Preparation. Gold-coated silicon tips were cleaned in H_2SO_4, H_2O, H_2O, and EtOH (each step 1 min) and dried in an N_2 stream before being placed into a 1 mM ethanolic solution of the respective carboranethiols. After 12−18 h, the tips were taken out of the solution, washed with hexane and ethanol to remove any unbound thiols, and dried in an N_2 stream before use for AFM experiments.

Lipid Monolayer Preparation. For monolayer deposition the cationic lipid dimethyldioctadecylammonium(bromide salt) (DODA, also known as DDAB or DODAB) was suspended in a mixture of chloroform and methanol (7:3 volume fractions). The monolayer was deposited using the Langmuir−Blodgett technique[32] on a freshly cleaved mica surface glued to a glass-slide along with an O-ring using UV-curable glue (Norland Adhesive, NOA81). The layer of DODA was transferred to the mica surface at the rate of 0.5 mm/min, at a lateral pressure of 40 mN/m and an area of 42 Å^2 per molecule.

SFA Measurements. SFA normal force measurements were performed at 23 °C in a cleanroom using the SFA 2000 model obtained from SurForce LLC (Santa Barbara, U.S.A.).[21] Mica sheets used in these experiments were hand-cleaved to provide sheets with an area of several (typically 5−10) cm^2 and uniform thicknesses ranging from 2 to 5 μm. The edges of these sheets were melt-cut with a hot platinum wire. PVD back-silvered mica sheets were cut into smaller pieces using a surgical blade, and were then glued to cylindrical silica disks with a nominal radius of curvature R = 2 cm, using a UV curable glue (Norland Adhesives, NOA81). Atomically smooth Au films and SAM-modified SFA discs were prepared by template stripping as previously described.[7] The contact reference was measured in dry argon between mica and gold. D = 0 is referenced to the contact between clean Au and mica. A spring constant of ∼800 N/m was used for force measurements. The work of adhesion, W_{ADH} was calculated using $F_{ADH} = 1.5\pi W_{ADH}$.

Photoelectron Spectroscopy (XPS). XPS measurements were performed with a Quantum 2000 (Physical Elecronics) using pass-energies of 29.35 eV. All XPS spectra were measured with the "high-power mode" of the used machine. In this mode photoelectrons are generated by continuously scanning a $100 \times 100\ \mu m^2$ sized X-ray spot (100 W) over an area of $100 \times 1000\ \mu m^2$ in order to minimize X-ray damage to the sample. All data were recorded with a pass-energy of 29.35 eV, and a spectral resolution of 0.25 eV. To obtain a good signal-to-noise ratio 10 sweeps for the Au 4f signal, and 45 sweeps for all other signal were used. All measurements are aligned using the Au 2p signal.

Water Contact Angle. A custom-built contact angle goniometer was used for the contact angle measurements. A motorized syringe device (model 33, Harvard Apparatus) was used to dispense pure water drops through a syringe needle onto the substrate. The advancing and receding contact angles were measured by increasing the drop volume at a constant volumetric flow rate. The silhouette of the drop was recorded using a video camera system. All experiments were performed at 23 °C.

Fitting Equations for Modeling Force–Distance Profiles. Here, we use the Hydra model[28] for a sphere on flat geometry that describes the interaction between hydrophobic/hydrophilic interactions as a linear superposition of van der Waals (VDW) and hydration/hydrophobic forces as follows:

$$\frac{F(D)}{R} = -\frac{A_H(D)}{6} - 4\pi\gamma_i \mathrm{Hy}\, e^{-(D - D_0)/\lambda_{Hy}} \quad (\mathrm{mN/m}) \qquad (1)$$

with the probe radius R and the interfacial tension γ_i. D_0 is the plane of origin of the respective forces, and is necessary for SFA data, where $D = 0$ does not coincide with the plane of origin of the interaction forces (see again Figure 1 for definition of $D = 0$). In SFA, $D = 0$ is directly measurable as a final hardwall at high compression. Also, the exponential decay length λ_{Hy} is directly measurable from the slope in a semilog plot and is as such not a fitting variable, but rather an experimental observable. The latter two parameters may depend directly on the probe radius.[30,33] Hydra, Hy, is the recently introduced parameter quantifying the fraction of hydrophobic surface area. Hy < 0 indicates a hydrophobic interaction with a water depletion layer at the extended interface. While Hy > 0 indicates an overall hydrophilic interaction with water and/or ions strongly adsorbed at an interface. Using a distance-dependent Hamaker constant $A_H(D)$ takes into account that long-range VDW forces are dominated by the Au|mica dispersion, while short-range VDW forces are dominated by the adsorbed organic thin films (SAM and lipid monolayer). For an asymmetric system $A_H(D)$ can be approximated using combining rules[25] as follows:

$$A_H(D) \approx \frac{A_{132}}{(D - D_0)^2} + \frac{A_{121}}{(D - D_0 + T_{TOT})^2} \quad (\mathrm{J}) \qquad (2)$$

with $A_{132} = 7.1 \times 10^{-21}$ (J) and $A_{121} = 3.4 \times 10^{-20}$ (J) quantifying the Hamaker constant for an organic thin-film interacting across the medium with mica, and for gold interacting with mica across an organic thin film, respectively. The values are fixed and taken from literature.[23] $T_{TOT} = T_{SAM} + T_{LM}$ is the total thickness of the combined organic thin films which can be directly extracted from SFA measurements. For a full DLVO interaction plus a hydrophobic/hydrophilic interaction an additional term in eq 1 taking into account electric double layer repulsions would be necessary. Here, however, the SFA data at extended surfaces for the **M1** case (extremely long ranged interaction) cannot be fit with the standard electric double layer model. All other experiments did not show any significant electrostatic interaction, and forces were dominated by the hydration/hydrophobic interaction and a linear superposition of VDW forces.

Conflict of Interest: The authors declare no competing financial interest.

Acknowledgment. Surface forces apparatus and contact angle experiments have been supported by Department of Energy, Division of Materials Sciences under Award No. DE-FG02-87ER-45331. M.V. acknowledges financial support through a Marie Curie International Outgoing Fellowship within the seventh European Community Framework Program under Award No. IOF-253079. T.B. acknowledges financial support through a Humboldt research fellowship.

Supporting Information Available: Back of an envelope calculation of carborane-dipole/water-dipole interaction energy. Additional table of the XPS derived energy data of **M1** SAM on gold and **M9** SAM on gold. This material is available free of charge *via* the Internet at http://pubs.acs.org.

REFERENCES AND NOTES

1. Donaldson, S. H., Jr.; Valtiner, M.; Gebbie, M. A.; Harada, J.; Israelachvili, J. N. Interactions and Visualization of Biomimetic Membrane Detachment at Smooth and Nano-Rough Gold Electrode Surfaces. *Soft Matter* **2013**, *9*, 5231–5238.
2. Han, X. T.; Qin, M.; Pan, H.; Cao, Y.; Wang, W. A Versatile "Multiple Fishhooks" Approach for the Study of Ligand-Receptor Interactions Using Single-Molecule Atomic Force Microscopy. *Langmuir* **2012**, *28*, 10020–10025.
3. Duzgunes, N.; Nir, S. Mechanisms and Kinetics of Liposome–Cell Interactions. *Adv. Drug Delivery Rev.* **1999**, *40*, 3–18.
4. Shefy-Peleg, A.; Foox, M.; Cohen, B.; Zilberman, M. Novel Antibiotic-Eluting Gelatin-Alginate Soft Tissue Adhesives for Various Wound Closing Applications. *Int. J. Polym. Mater. Polym. Biomater.* **2014**, *63*, 699–707.
5. An, J. H.; Huynh, N. T.; Jeon, Y. S.; Kim, J. H. Surface Modification Using Bio-inspired Adhesive Polymers Based on Polyaspartamide Derivatives. *Polym. Int.* **2011**, *60*, 1581–1586.
6. Zang, D. M.; Cao, D. K.; Zheng, L. M. Strontium and Barium 4-Carboxylphenylphosphonates: Hybrid Anti-corrosion Coatings for Magnesium Alloy. *Inorg. Chem. Commun.* **2011**, *14*, 1920–1923.
7. Valtiner, M.; Donaldson, S. H.; Gebbie, M. A.; Israelachvili, J. N. Hydrophobic Forces, Electrostatic Steering, and Acid-Base Bridging between Atomically Smooth Self-Assembled Monolayers and End-Functionalized Pegolated Lipid Bilayers. *J. Am. Chem. Soc.* **2012**, *134*, 1746–1753.
8. Love, J. C.; Estroff, L. A.; Kriebel, J. K.; Nuzzo, R. G.; Whitesides, G. M. Self-Assembled Monolayers of Thiolates on Metals as a Form of Nanotechnology. *Chem. Rev.* **2005**, *105*, 1103–1169.
9. Ulman, A. Formation and Structure of Self-Assembled Monolayers. *Chem. Rev.* **1996**, *96*, 1533–1554.
10. Mutin, P. H.; Guerrero, G.; Vioux, A. Hybrid Materials from Organophosphorus Coupling Molecules. *J. Mater. Chem.* **2005**, *15*, 3761–3768.
11. Mastropietro, D. J.; D, W. A. Forces between Hydrophobic Solids in Concentrated Aqueous Salt Solution. *Phys. Rev. Lett.* **2012**, *108* (106101), 1–4.
12. Donaldson, S. H., Jr.; Lee, C. T., Jr.; Chmelka, B. F.; Israelachvili, J. N. General Hydrophobic Interaction Potential for Surfactant/Lipid Bilayers from Direct Force Measurements between Light-Modulated Bilayers. *Proc. Natl. Acad. Sci. U.S.A.* **2011**, *108*, 15699–15704.
13. Israelachvili, J.; Pashley, R. The Hydrophobic Interaction Is Long-Range, Decaying Exponentially with Distance. *Nature* **1982**, *300*, 341–342.
14. Meyer, E. E.; Lin, Q.; Hassenkam, T.; Oroudjev, E.; Israelachvili, J. N. Origin of the Long-Range Attraction between Surfactant-Coated Surfaces. *Proc. Natl. Acad. Sci. U.S.A.* **2005**, *102*, 6839–6842.
15. Perkin, S.; Kampf, N.; Klein, J. Long-Range Attraction between Charge-Mosaic Surfaces across Water. *Phys. Rev. Lett.* **2006**, *96*, 038301.
16. Hohman, J. N.; Z, P.; Morin, E. I.; Han, P.; Kim, M.; Kurland, A. R.; McClanahan, P. D.; Balema, V. P.; Weiss, P. S. Self-Assembly of Carboranethiol Isomers on Au{111}: Intermolecular Interactions Determined by Molecular Dipole Orientations. *ACS Nano* **2009**, *3*, 527–534.

17. Hohman, J. N.; Claridge, S. A.; Moonhee, K.; Weiss, P. S. Cage Molecules for Self-Assembly. *Mater. Sci. Eng. R* **2010**, *70*, 188–208.
18. Belman, N.; Jin, K.; Golan, Y.; Israelachvili, J. N.; Pesika, N. S. Origin of the Contact Angle Hysteresis of Water on Chemisorbed and Physisorbed Self-Assembled Monolayers. *Langmuir* **2012**, *28*, 14609–14617.
19. Tomáš Baše, Z. B.; Plzák, Zbynèk; Tomáš, Grygar; Jaromír Plešek, M. J. C.; Václav, Malina; Jan, Šubrt; Jaroslav Bohácek, V.; Otomar, Kríž Carboranethiol-Modified Gold Surfaces. A Study and Comparison of Modified Cluster and Flat Surfaces. *Langmuir* **2005**, *21*, 7776–7785.
20. Israelachvili, J. N. Thin-Film Studies Using Multiple-Beam Interferometry. *J. Colloid Interface Sci.* **1973**, *44*, 259–272.
21. Israelachvili, J. N.; Min, Y.; Akbulut, M.; Alig, A.; Carver, G.; Greene, W.; Kristiansen, K.; Meyer, E.; Pesika, N.; Rosenberg, K.; Zeng, H. Recent Advances in the Surface Forces Apparatus (SFA) Technique. *Rep. Prog. Phys.* **2010**, *73*, 036601.
22. Alcantar, N.; Israelachvili, J.; Boles, J. Forces and Ionic Transport between Mica Surfaces: Implications for Pressure Solution. *Geochim. Cosmochim. Acta* **2003**, *67*, 1289–1304.
23. Israelachvili, J. N. *Intermolecular and Surface Forces*; 3rd ed.; Academic Press: Burlington, MA, 2011.
24. The contact angle of DODA changes from 100° to 65° over the course of 60 min, indicating that DODA molecules at the mica surface are overturning.
25. Donaldson, S. H., Jr.; Das, S.; Gebbie, M. A.; Rapp, M.; Jones, L. C.; Roiter, Y.; Koenig, P. H.; Gizaw, Y.; Israelachvili, J. N. Asymmetric Electrostatic and Hydrophobic–Hydrophilic Interaction Forces between Mica Surfaces and Silicone Polymer Thin Films. *ACS Nano* **2013**, *7*, 10094–10104.
26. Hammer, M. U.; Anderson, T. H.; Chaimovich, A.; Shell, M. S.; Israelachvili, J. The Search for the Hydrophobic Force Law. *Faraday Discuss.* **2010**, *146*, 299–308.
27. Meyer, E. E.; Rosenberg, K. J.; Israelachvili, J. Recent Progress in Understanding Hydrophobic Interactions. *Proc. Natl. Acad. Sci. U.S.A.* **2006**, *103*, 15739–15746.
28. Donaldson, S. H.; Røyne, A.; Kristiansen, K.; Rapp, M. V.; Das, S.; Gebbie, M. A.; Lee, D. W.; Stock, P.; Valtiner, M.; Israelachvili, J. Developing a General Interaction Potential for Hydrophobic and Hydrophilic Interactions. *Langmuir* **2014**, 10.1021/la502115g.
29. Valtiner, M.; Grundmeier, G. Single Molecules as Sensors for Local Molecular Adhesion Studies. *Langmuir* **2010**, *26*, 815–820.
30. Huang, D. M.; Chandler, D. Temperature and Length Scale Dependence of Hydrophobic Effects and Their Possible Implications for Protein Folding. *Proc. Natl. Acad. Sci. U.S.A.* **2000**, *97*, 8324–8327.
31. Tabor, R. F.; Wu, C.; Grieser, F.; Dagastine, R. R.; Chan, D. Y. C. Measurement of the Hydrophobic Force in a Soft Matter System. *J. Phys. Chem. Lett.* **2013**, *4*, 3872–3877.
32. Zasadzinski, J. A.; Viswanathan, R.; Madsen, L.; Garnaes, J.; Schwartz, D. K. Langmuir–Blodgett Films. *Science* **1994**, *263*, 1726–1733.
33. Chaimovich, A.; Shell, M. S. Anomalous Waterlike Behavior in Spherically-Symmetric Water Models Optimized with the Relative Entropy. *Phys. Chem. Chem. Phys.* **2009**, *11*, 1901–1915.